

#### **PAPER**

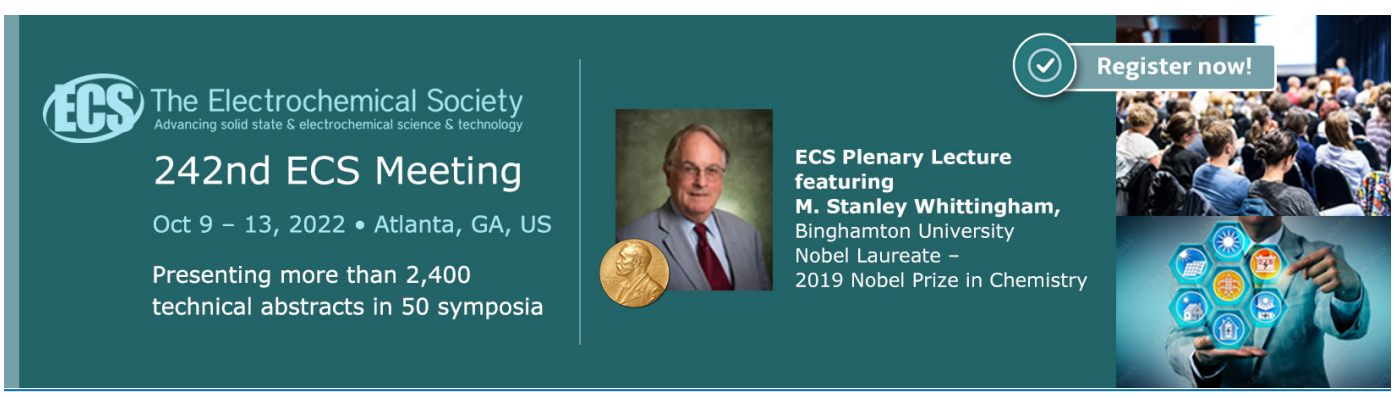
# Nucleation efficiency of nuclear recoils in bubble chambers

To cite this article: D. Durnford et al 2022 JINST 17 C01030

View the article online for updates and enhancements.

## You may also like

- Xenon bubble chambers for direct dark matter detection
  C. Levy, S. Fallon, J. Genovesi et al.
- Direct detection of WIMP dark matter: concepts and status Marc Schumann
- <u>Dark matter direct-detection experiments</u> Teresa Marrodán Undagoitia and Ludwig Rauch





RECEIVED: October 31, 2021 Accepted: November 18, 2021 Published: January 7, 2022

LIGHT DETECTION IN NOBLE ELEMENTS (LIDINE 2021) 14–17 SEPTEMBER, 2021 ONLINE

# Nucleation efficiency of nuclear recoils in bubble chambers

#### D. Durnford\* and M.-C. Piro on behalf of SBC and PICO collaborations

Department of Physics, University of Alberta, Edmonton, Alberta, T6G 2R3, Canada

E-mail: ddurnfor@ualberta.ca

ABSTRACT: Bubble chambers using liquid xenon (and liquid argon) have been operated (resp. planned) by the Scintillating Bubble Chamber (SBC) collaboration for GeV-scale dark matter searches and  $CE\nu NS$  from reactors. This will require a robust calibration program of the nucleation efficiency of low-energy nuclear recoils in these target media. Such a program has been carried out by the PICO collaboration, which aims to directly detect dark matter using  $C_3F_8$  bubble chambers. Neutron calibration data from mono-energetic neutron beam and Am-Be source has been collected and analyzed, leading to a global fit of a generic nucleation efficiency model for carbon and fluorine recoils, at thermodynamic thresholds of 2.45 and 3.29 keV. Fitting the many-dimensional model to the data (34 free parameters) is a non-trivial computational challenge, addressed with a custom Markov Chain Monte Carlo approach, which will be presented. Parametric MC studies undertaken to validate this methodology are also discussed. This fit paradigm demonstrated for the PICO calibration will be applied to existing and future scintillating bubble chamber calibration data.

KEYWORDS: Analysis and statistical methods; Detector modelling and simulations I (interaction of radiation with matter, interaction of photons with matter, interaction of hadrons with matter, etc.); Liquid detectors; Scintillators, scintillation and light emission processes (solid, gas and liquid scintillators)

*Corres	ponding	author
Corres	ponung	auunoi.

Co	ntents	
1	Introduction	1
2	PICO data and simulations	2
3	Analysis and results	2
4	Measurement with a LXe bubble chamber	5
5	Conclusion	6

#### 1 Introduction

The search for dark matter (DM) and coherent elastic neutrino nucleus scattering (CEvNS) through the observation of low-energy nuclear recoils requires detector technologies designed to be sensitive to sub-keV thresholds while having a high power of background rejection [1]. The Scintillating Bubble Chamber (SBC) experiment uses novel low-background detectors with noble liquids and a 100 eV energy threshold, aimed at detecting low-mass (0.7–7 GeV/c²) DM interactions and CEvNS from reactor neutrinos [2, 3]. The advantage of such technology is that it combines the electron recoil discrimination of bubble chambers and energy reconstruction from scintillation light. The first demonstration of a scintillating bubble chamber was a successfully operated 30 g liquid xenon (LXe) bubble chamber [4], establishing noble-liquid bubble chambers as a promising new technology to reach these physics goals. However, understanding the detector response and nucleation efficiency to low-energy nuclear recoils is necessary for the interpretation of experimental results.

Bubble chambers use super-heated liquids to search for rare, low-energy nuclear recoils. The threshold energy is set by the pressure/temperature conditions of the target fluid. Particle interactions with energy above threshold induce a small volume of liquid to rapidly transition into a vapor state. This nucleation can be observed optically with cameras, acoustically with piezo-electric transducers, or barometrically. The process of particle-induced bubble nucleation is typically described by Seitz's "hot spike" model [5], which predicts a threshold energy based on the to thermodynamic state (pressure and temperature) of the medium. However, it is well known from the PICO collaboration that the true threshold for nucleation deviates from the predicted Seitz "thermodynamic threshold" [6]. A new approach has been developed to determine the nucleation efficiency of nuclear recoils in super-heated liquids [7] with dedicated neutron calibrations carried out by the PICO collaboration. In this paper, the preliminary results will be presented for both conventional and noble liquids bubble chambers. <sup>1</sup>

<sup>&</sup>lt;sup>1</sup> Publication with more details in preparation.

#### 2 PICO data and simulations

Dedicated neutron calibrations over the past 6 years at various thermodynamic thresholds ranging from 2.1 keV to 3.9 keV as summarized in table 1, have been performed by the PICO collaboration to measure the nucleation efficiency in super-heated  $C_3F_8$ . This includes experiments done with two detectors (PICO-0.1L [8] and PICO-2L [6]), with neutron sources (Am-Be and Sb-Be compound sources) as well as neutron beams generated with a TANDEM accelerator at the Université de Montréal [9]. The proton beam is used to produce mono-energetic neutron with energies of 50, 61, and 97 keV obtained with a vanadium target via the reaction  $^{51}V(p, n)^{51}Cr$  [10]. Fluorine cross-section resonances at 50 and 97 keV, and an anti-resonance 61 keV, break the degeneracy between neutron scattering on carbon and fluorine [8]. Neutrons can also scatter multiple times in the detector as they slow down creating multiple bubble events, constraining the nucleation efficiency at several recoil energies simultaneously. Each experiment was simulated using Geant4 [11] or MCNPX-Polimi [12] to provide the spectrum of energy depositions on each target atom species in the corresponding chamber, for all multiplicities (number of bubbles per event).  $^{3}$ He counters were deployed to measure source strengths and normalize the simulated spectra.

**Table 1.** PICO neutron calibration data sets used in this analysis, listing the detector and Seitz thresholds used, as well as bubble multiplicities (number of bubbles per event) included in the analysis.

Dataset	Detector	Thresholds (keV)	Multiplicity
97 keV Beam	PICO-0.1 (2013, 2014)	3.0, 3.2, 3.6	1,2,3+
61 keV Beam	PICO-0.1 (2013, 2014)	2.9, 3.1, 3.6	1,2,3+
50 keV Beam	PICO-0.1 (2014)	2.5, 3.5	1,2,3+
SbBe	PICO-0.1	2.1, 2.6, 3.2	2,3+
AmBe	PICO-2L	3.2	1,2,3,4,5,6,7+

### 3 Analysis and results

In the absence of an *a priori* physical model for the shape of the nucleation efficiency curve, a piece-wise linear function is used, with 4 linear segments between 5 fixed efficiency knots at 0, 0.2, 0.5, 0.8, and 1. The recoil energies at which these efficiency knots are reached are the free parameters of the model. There are separate nucleation efficiency curves for carbon and fluorine. To span the range of thermodynamic thresholds in the data, two threshold "fence-posts" are defined at 2.45 keV and 3.29 keV. With most of the data clustered around these energies, a linear scaling to the nearest of the two fence-posts is used to interpolate/extrapolate for different thermodynamic states. In total, this yields a model with 4 nucleation efficiency curves with 20 free parameters. Additionally, nuisance parameters are added to account for systematics for each of the experiments, including uncertainties on beam fluxes and source strengths, geometry, and pressure/temperature conditions for a total of 34 parameters. The associated likelihood function for this model, with

contributions summed over each experiment i and events with j bubbles, is given as

$$\log \mathcal{L} = \sum_{i} \sum_{j} \left( -\nu_{i,j}(\{x_{n,p}\}, \{s_k\}) + k_{i,j} + k_{i,j} \log \left( \frac{\nu_{i,j}(\{x_{n,p}\}, \{s_k\})}{k_{i,j}} \right) \right) - \sum_{k} \frac{s_k^2}{2}.$$
(3.1)

Here  $k_{i,j}$  is the number of bubbles observed in each case, and  $v_{i,j}$  is the expected number of bubbles for a given input set of parameters defining a set of efficiency curves x(n,p), which are then applied to the simulated spectra. The nuisance parameters are included in the final term, with  $s_k$  being a scaling factor for the expected standard deviation of each nuisance parameter.

To fit this high-dimensional model, a Markov Chain Monte Carlo (MCMC) [13] is a natural choice of optimization strategy, but for which exploring the likelihood function is still computationally expensive. A modified approach was developed [7] wherein the MCMC is run for a small number of steps (5–10), after which the random walkers are stopped and the cumulative samples are binned in each parameter. The maximum likelihood samples in each bin are then used as starting points for a new set of MCMC walkers. This process is repeated iteratively until convergence is reached. This forces the MCMC to preferentially explore the boundary of the likelihood function, leading to more efficient computation of the maximum-likelihood point and uncertainty bands (assuming a roughly Gaussian likelihood [14]). Convergence was considered to be achieved when the maximum likelihood and span of samples within  $1\sigma$  of the maximum do not deviate by more than 0.1% for 25 consecutive MCMC iterations. The results of the fit to the data are shown in figure 1. It is evident that the nucleation curves deviate significantly from their respective Seitz thresholds, more so for carbon than for fluorine (as expected, since dE/dx will be lower for lighter atoms). This is consistent with the original results obtained with this calibration data [15].

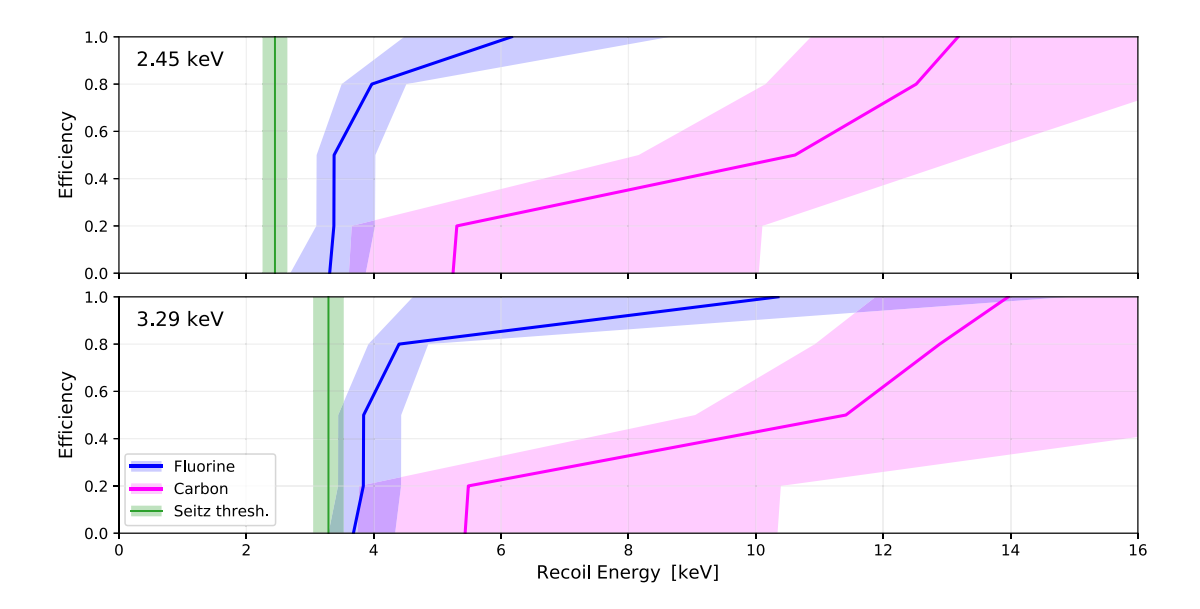


**Figure 1.** Nucleation efficiency curves obtained for the PICO calibration data, showing the best fit curves and  $1\sigma$  error bands for fluorine and carbon (blue and magenta respectively), and for both thermodynamic thresholds (2.45 keV above, 3.29 keV below) indicated by the green bands.

To further study the efficacy of this empirical model for nucleation efficiency and fit-strategy, a parametric Monte Carlo study was carried out. 25 simulated data sets were constructed using the best-fit model to the data, and fit with the exact same fitting procedure. The first conclusion from this study is confirmation that the convergence criteria used is sufficient. Another result is the ability to interpret the  $\chi^2$  value of the best-fit model ( $\chi^2 = -2 \times \log \mathcal{L}$ ) as a goodness-of-fit value. This is non-trivial as the number of degrees of freedom of the fit is confounded by the correlations between many of the parameters. Using the distribution of  $\chi^2$  for the MC data sets, the effective number of degrees of freedom of the fit was found to be 46, giving the fit to the real data a one-sided p-value of 0.189, proving that the data is reasonably represented by the empirical model used.

Finally, the MC study can be used to check for systematic biases in the model/fit paradigm. Comparing the average MC fit result to the best-fit to the data (the MC truth model) reveals small but persistent offsets for some of the 20 parameters of interest. However, the fit bias for a given parameter  $\theta_i$  may not be a constant offset, but rather a function of that parameter  $\theta_i$  or any other  $\theta_{j,j\neq i}$ . Therefore, a bias study only carried out for MC data generated from one input model only measures the fit bias of each parameter at one point in the parameter space. To better characterize the fit bias, an additional 25 MC data sets were generated from efficiency curves drawn randomly from within the  $1\sigma$  band of the real data result, and fit using the same procedure. The results were used to measure the fit bias in the 20 parameters of interest as a function of all 20 parameters, fit with a first-order polynomial. This yields 400 constraints of the form  $\theta_{i_{fit}} = \theta_{i_{true}} + B_{ij}(\theta_{j_{true}})$  where  $B_{ij}$  is the bias in parameter i as a function of parameter j. This was used to construct a likelihood function for the true values of the parameters:

$$\log \mathcal{L}(\{\theta_{\text{fit}}\} \mid \{\theta_{\text{true}}\}) = \sum_{j} \sum_{i} \log P\left(\theta_{i_{\text{fit}}} = \theta_{i_{\text{true}}} + B_{ij}\left(\theta_{j_{\text{true}}}\right)\right). \tag{3.2}$$

Maximizing this yields a bias-corrected fit result, which is shown alongside the original in figure 2. Despite this being a low-powered study, it demonstrates the robustness of the model and fitting approach used and that any systematic biases in this approach are not significant.<sup>1</sup>

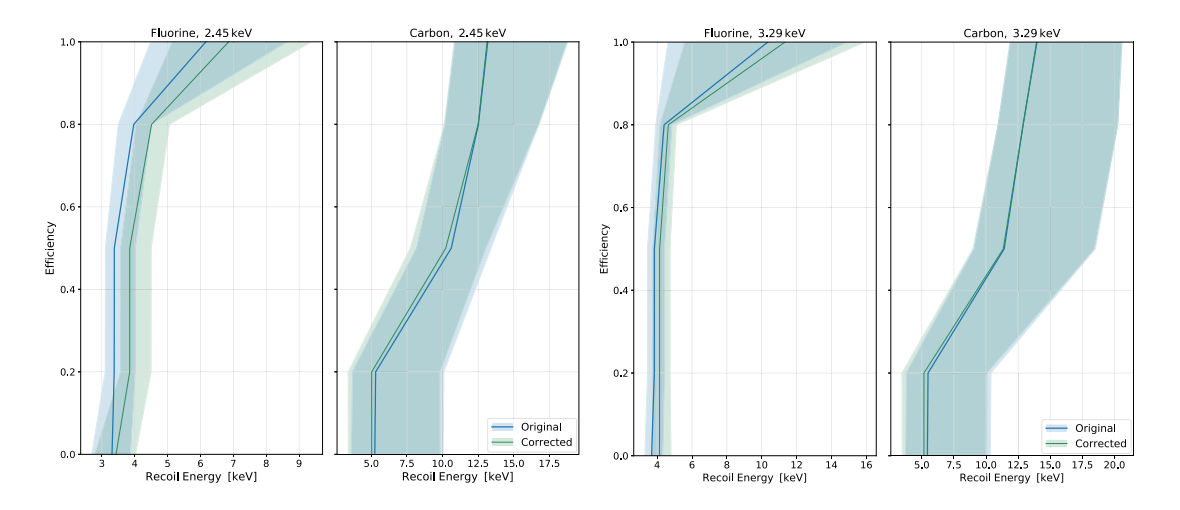


**Figure 2.** Comparison between the original nucleation efficiency curves for PICO (blue) and the biascorrected results (green), for both thermodynamic thresholds (2.45 keV left, 3.29 keV right).

### 4 Measurement with a LXe bubble chamber

The techniques developed and applied to the PICO calibration data are directly applicable to other bubble chamber experiments such as the SBC collaboration's LXe prototype chamber [4]. Nuclear recoil calibration data was taken with a <sup>252</sup>Cf neutron source and various photo-neutron sources. To date, a Geant4 simulation [11] has been produced describing the <sup>252</sup>Cf experiment, allowing for an analysis with this data, taken at thermodynamic thresholds of 0.9, 1.19, 1.89, and 2.06 keV. The scintillation signal was used to remove the background signal (the scintillation yield is higher for electronic recoils). As with the PICO analysis, a piece-wise linear model is used for the nucleation efficiency curves, with thermodynamic threshold fence-posts at 0.9 and 2 keV, and for a single target species. The same interpolation scheme is used for data sets with different thermodynamic states, and nuisance parameters are included to incorporate experimental systematics. The same iterative MCMC approach [7] and convergence criteria are used, with the resulting fit shown in figure 3. As with the C<sub>3</sub>F<sub>8</sub> result, these experimental nucleation efficiency curves for LXe deviate significantly from their theoretical Seitz thresholds, albeit with significant uncertainty. Although this initial analysis is promising in terms of demonstrating sensitivity to ~1 keV recoils, future work will incorporate the photo-neutron calibration data to better constrain the nucleation efficiency of LXe bubble chambers.

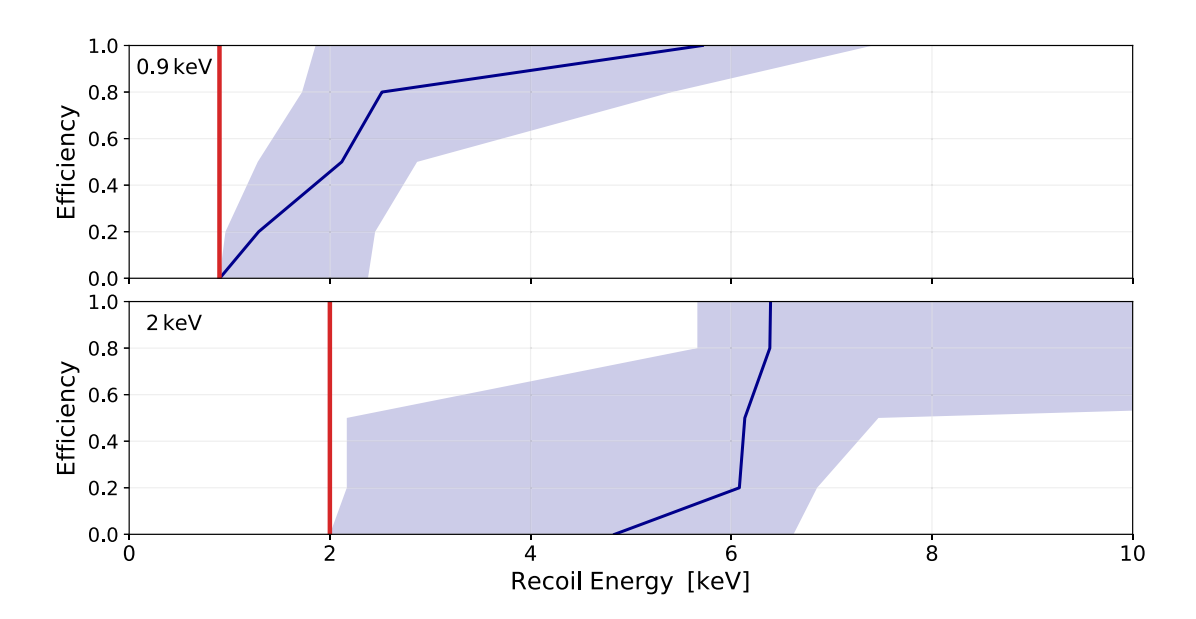


**Figure 3.** Preliminary nucleation efficiency results in LXe (best-fit and  $1\sigma$  error in blue), for thermodynamic thresholds of 0.9 keV and 2 keV (red).

#### 5 Conclusion

A method to extract the nucleation efficiency from neutron calibrations has been developed and applied to PICO data, yielding nucleation efficiency curves for  $C_3F_8$  compatible with previously published results [15]. This includes a flexible model for nucleation efficiency that is dependent on thermodynamic state and target atom species, as well as a novel MCMC optimization technique to overcome computational challenges. The robustness of this approach has been tested with simulated data sets, demonstrating that any systematic biases are small and correctable, and that the model adequately represents the PICO data. This method can be applied to other bubble chamber target medium, with preliminary results shown for LXe, and will be used by the SBC collaboration for future liquid noble bubble chamber experiments.

## Acknowledgments

This research was undertaken, in part, thanks to funding from the Arthur B. McDonald Canadian Astroparticle Physics Research Institute and the Natural Sciences and Engineering Research Council of Canada. We gratefully acknowledge the support of Compute Canada for providing the computing resources required to undertake this work. We also acknowledge the SBC and PICO collaborations.

#### References

- [1] A.J. Anderson et al., *Coherent neutrino scattering in dark matter detectors, Phys. Rev. D* **84** (2011) 013008.
- [2] P. Giampa, *The scintillating bubble chamber (SBC) experiment for dark matter and reactor CEvNS*, *PoS* **ICHEP2020** (2021) 632.
- [3] L.J. Flores et al., *Physics reach of a low threshold scintillating argon bubble chamber in coherent elastic neutrino-nucleus scattering reactor experiments*, *Phys. Rev. D* **103** (2021) 091301.
- [4] D. Baxter et al., First demonstration of a scintillating xenon bubble chamber for detecting dark matter and coherent elastic neutrino-nucleus scattering, Phys. Rev. Lett. 118 (2017) 231301.
- [5] F. Seitz, On the theory of the bubble chamber, Phys. Fluids 1 (1958) 2.
- [6] C. Amole et al., *Dark matter search results from the PICO-2L C*<sub>3</sub>*F*<sub>8</sub> *bubble chamber, Phys. Rev. Lett.* **114** (2015) 231302.
- [7] M. Jin, Measurements and Analysis of the Sensitivity of Superheated C<sub>3</sub>F<sub>8</sub> Bubble Chambers to Interactions from WIMP Dark Matter, ProQuest Dissertations Publishing (2019).
- [8] F. Girard, Calibration of the PICO-0.1 bubble chamber and development of coated inner vessels for dark matter search, https://zone.biblio.laurentian.ca/handle/10219/2830 (2017).
- [9] R.J. Van de Graaff, Tandem electrostatic accelerators, Nucl. Instrum. Meth. 8 (1960) 195.
- [10] J.H. Gibbons, R.L. Macklin and H.W. Schmitt, <sup>51</sup>V(p, n)<sup>51</sup>Cr reaction as a 5- to 120-keV neutron source, Phys. Rev. **100** (1955) 167.
- [11] S. Agostinelli et al., Geant4 a simulation toolkit, Nucl. Instrum. Meth. A 506 (2003) 250.

- [12] S.A. Pozzi, E. Padovani and M. Marseguerra, MCNP-PoliMi: a Monte-Carlo code for correlation measurements, Nucl. Instrum. Meth. A 513 (2003) 550.
- [13] D. Foreman-Mackey, D.W. Hogg, D. Lang and J. Goodman, emcee: the MCMC hammer, Publ. Astron. Soc. Pac. 125 (2013) 306.
- [14] G. Cowan, Statistical Data Analysis, Oxford University Press (1998).
- [15] C. Amole et al., Dark matter search results from the complete exposure of the PICO-60  $C_3F_8$  bubble chamber, Phys. Rev. D 100 (2019) 022001.